*27th EPS Conference on Contr. Fusion and Plasma Phys. Budapest, 12-16 June 2000 ECA Vol.* **24B** *(2000) 229 -232*

# Investigation of Experimental Equilibrium Domain in NSTX Ohmic Plasmas

S. A. Sabbagh[1], M. Bell[2], M. Bitter[2], D. Gates[2], S. M. Kaye[2], L. L. Lao[3], R. Maingi[4], R. Maqueda[5], E. Mazzucato[2], J. Menard[2], D. Mueller[2], F. Paoletti[1], S. Paul[2], D. Stutman[6], G. A. Wurden[5], and the NSTX Research Team

[1] *Department of Applied Physics and Applied Mathematics, Columbia University, New York, NY, USA*
[2]*Princeton Plasma Physics Laboratory, Princeton University, Princeton, NJ, USA*
[3]*General Atomics, San Diego, CA, USA*
[4]*Oak Ridge National Laboratory, Oak Ridge, TN, USA*
[5]*Los Alamos National Laboratory, Los Alamos, NM, USA*
[6]*Johns Hopkins University, Baltimore, MD, USA*

## 1. Introduction:

The spherical torus [1] (ST), a variant of the standard tokamak, offers several potential advantages as a fusion energy reactor[2]. The ST concept maximizes field utilization and minimizes device size by adopting a low aspect ratio. The most attractive ST reactor designs require operation at both high fusion power and high bootstrap current fraction. The latter characteristic yields a strong dependence of fusion power density on normalized beta, $P_f/V \sim \beta_N^4$, underlining the importance of maximizing this parameter, as well as toroidal beta.

Stable, experimental high $\beta_N \equiv 10^8 \langle \beta_t \rangle aB_0/I_p < 6$ ST equilibria have been demonstrated in the START [3] device. The promising results obtained in this relatively small scale machine (plasma current, $I_p \leq 0.3$ MA) have encouraged the recent construction and initial operation of proof-of-principle ST devices such as MAST [4] and the National Spherical Torus Experiment (NSTX) [5]. These machines are capable of operating with increased $I_p$ equal to or exceeding 1 MA, and auxiliary heating power exceeding 10 MW.

In any new device, a primary goal is to establish reproducible plasma configurations required for future experimentation. A basic and essential component of the analysis of these configurations is the accurate reconstruction of free-boundary MHD equilibria based on experimental measurements. This paper discusses the experimental production of the equilibrium configurations envisioned during the design phase of NSTX, their reconstruction from measurements, and the response of the equilibrium to observed plasma phenomena.

## 2. Establishing Ohmic equilibrium configurations in NSTX

NSTX has a major radius, $R_0 = 0.86$ m, and a midplane half-width of 0.7 m. The machine has been operated with an on-axis vacuum toroidal field, $B_0 \leq 0.3$ T, plasma current, $I_p \leq 1.0$ MA, and an average electron density up to 2.7 x$10^{19}$m$^{-3}$. Discharge pulse lengths at this current are typically 0.2s, and have been extended to 0.5s at lower $I_p$.

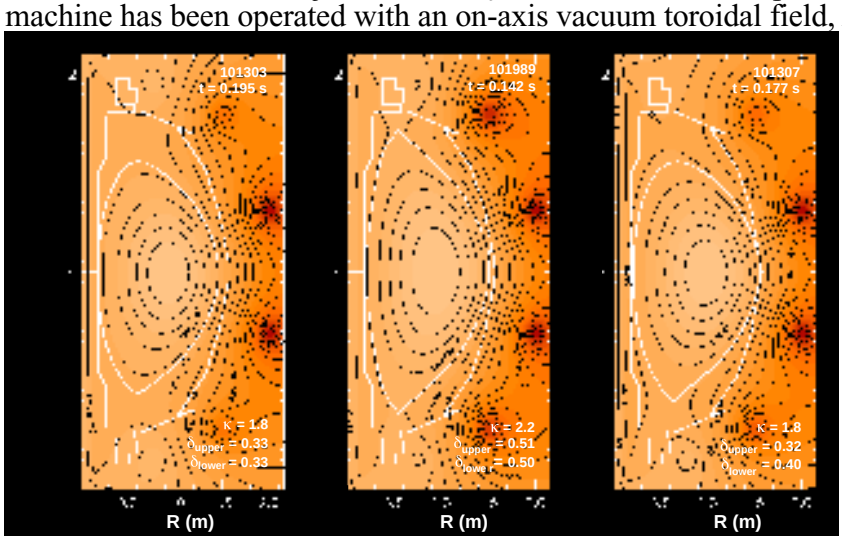


*Fig. 1. EFIT reconstructions of poloidal flux contours for limited, double-null, and lower single-null diverted equilibria.*

A key objective of the present work was the creation of a range of ohmic target plasmas suitable for neutral beam, high harmonic fast wave, and coaxial helicity injection, CHI [6]. Limiter, double-null, and lower single-null diverted configurations have been created (Fig. 1). Each

discharge was sustained at a nominally constant plasma current for a duration of greater than 100ms (approximately 5 energy confinement times, $\tau_E$). The plasmas shown in Fig. 1 have $I_p$ in the range 0.61 - 0.66 MA. Plasma elongation of $1.6 \le \kappa \le 2.0$ and triangularity in the range $0.25 \le \delta \le 0.45$ have been sustained, while maximum values of $\kappa = 2.3$ and $\delta = 0.6$ have been reached transiently. The largest plasma stored energy, $W_{tot}$ is attained in discharges with the highest values of plasma current, electron density, $n_e$, and plasma volume, $V$. The $\tau_E$ is observed to increase with increasing $n_e$. No specific configuration has yet proved superior in attaining maximum $W_{tot}$ or $\tau_E$.

The plasma current, and radial and vertical position are controlled by real-time feedback of the poloidal field coil currents while the plasma shape is currently controlled by pre-programming currents in the poloidal field shaping coils [7]. The evolution of the plasma equilibrium is then analyzed between shots with an automated version of the EFIT [8] code.

Figure 2 illustrates the evolution of plasma parameters for a discharge reaching $I_p = 0.98$ MA [9]. The approximate linear increase of the plasma internal inductance, $\ell_i$, as a function of time is observed during most discharges. Peak values of $\ell_i = 0.85$ are characteristic of 1 MA plasmas. Higher final values, $\ell_i = 1.3$, are usually reached at lower $I_p$. Because of the reduced resistance of the low aspect ratio vessel components, the proximity of the conducting structure, and the appreciable loop voltage (2-6 V), used during the $I_p$ increase, the induced currents flowing in the vacuum vessel wall and stabilizing conducting plates can be significant and are necessarily included in the reconstructions. During this discharge, the induced wall current varies between 0.25 and 0.3 MA from $t = 16$ ms (the vessel L/R time) until peak $I_p$ is reached. Plasma stored energy reaches 48 kJ +/- 10 kJ, (which equates to $\beta_t = 8.7\%$) at an ohmic input power of 2 MW at peak $W_{tot}$. The corresponding energy confinement time, $\tau_E$, reaches 25 ms at peak value, and is 18 ms at the time of peak stored energy.

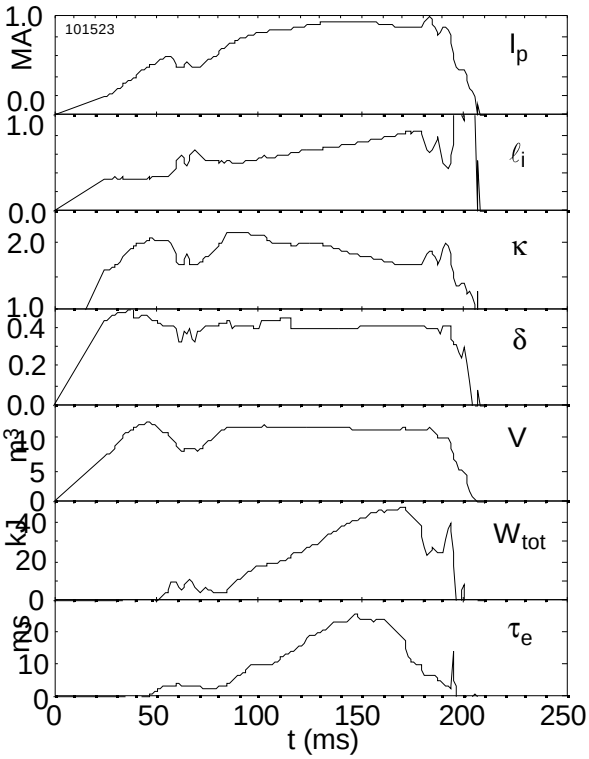


*Fig. 2: Time evolution of EFIT reconstructed plasma parameters for a 1 MA ohmic discharge. The interval between reconstructions is 1 ms.*

The 20% uncertainty in the plasma stored energy for the discharge shown in Fig 2 is estimated by examining the effect of systematic discrepancies between the plasma Rogowski and integrated dB/dt coil measurements. Figure 3 illustrates the variation of $W_{tot}$ as a function of the ratio between the reconstructed plasma current and the measured value input to EFIT. Based on the uncertainty in the measured $I_p$, it is expected that this ratio be between 0.97 - 0.98. However, ratios as high as 1 and as low as ~ 0.96 cannot be precluded by the results of the reconstructions. The response of $W_{tot}$ over this range is shown in Fig. 3 and used to produce the stated error estimate. Because of the small error bars on the input magnetic signals (see Section 4), it is expected that random error analysis will yield a lower

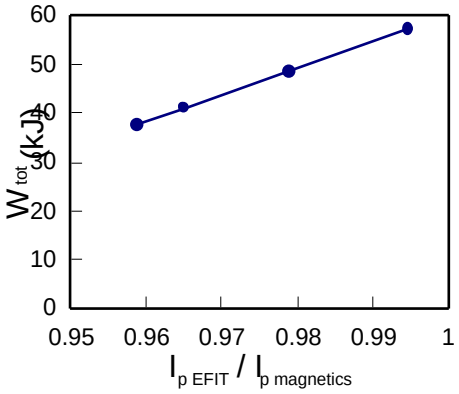


*Fig. 3: Response of $W_{tot}$ to variation in ratio of reconstructed to measured $I_p$.*

uncertainty in the plasma stored energy.

## 3. Observed plasma phenomena and equilibrium response

Highly time-resolved equilibrium reconstruction allows an examination of the equilibrium response to MHD instabilities and other plasma phenomena. Instabilities characterized as internal reconnection events (IREs) in previous ST experiments [10] have been observed in NSTX during both the increase and reduction of $I_p$. They can also occur somewhat randomly during the plasma evolution. These events are characterized by Mirnov oscillations, spikes in the $I_p$ evolution, $D_\alpha$ and Carbon-III light, and when sufficiently large, alteration of the plasma internal inductance and elongation. Figure 4 illustrates such events occurring during a 0.6 MA discharge. The first event occurring near the end of the rapid increase in $I_p$ leads to an increase in plasma internal inductance, $\Delta\ell_i$ = 0.1, indicating rapid current penetration and peaking of the current profile. A decrease in elongation of 0.3 also occurs, along with a corresponding drop in $I_p$. The second event occurs during the constant $I_p$ phase of the discharge with a similar perturbation in $\ell_i$ and $I_p$, but with less of a change in κ. Typically, a decrease in $\ell_i$ is observed as the event begins, sometimes with a slower precursor increase in the core radiated power, $P_{rad}$. The event terminates with a rapid decrease in $P_{rad}$ and a subsequent transient increase in $\ell_i$ (described further by Maingi, *et al.*)[11]. The third event heralds the start of the decrease in plasma current. As the loop voltage decreases to 2V at $t = 0.188$s, a relatively large IRE occurs, qualified by the larger perturbations in the relevant signals. A large, transient decrease of $\Delta\ell_i = -0.55$ occurs, with an increase in the elongation of 0.3. Animation of the poloidal flux contours show that both the boundary and the inner flux surfaces elongate in a similar fashion. The elongation at the plasma magnetic axis transiently increases by 0.5. A mild vertical oscillation begins after this event as $I_p$ decreases and $\ell_i$ increases, and the plasma finally terminates on the upper divertor plate after becoming vertically unstable.

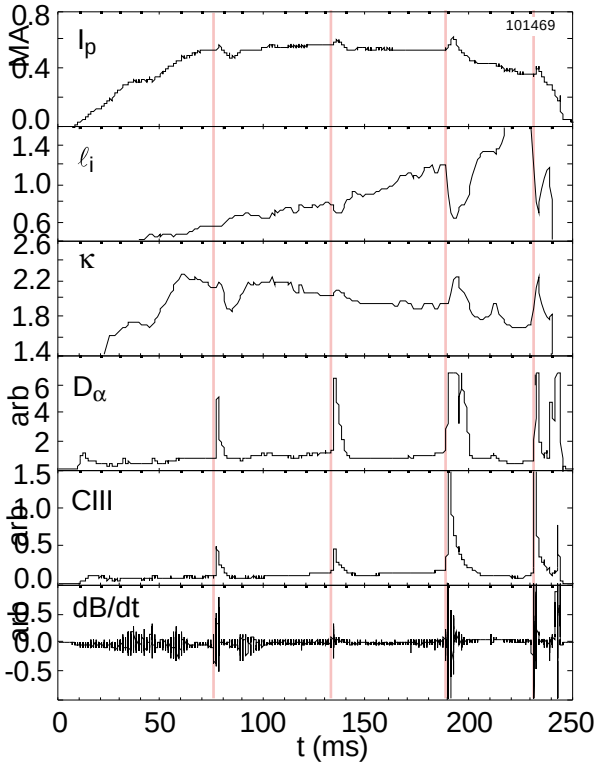


*Fig. 4: Plasma $\ell_i$ and shape response to internal reconnection events.*

Equilibria suitable for high-harmonic fast wave (HHFW) heating have been developed, and up to 2 MW of power has been injected into NSTX plasmas (detailed results presented by Swain, *et al.*)[12]. In experiments conducted using pulsed power (with a modulation frequency of 100 Hz), a similarly modulated response was observed in the plasma stored energy. The pulse period used was approximately one-half of the ohmic energy confinement time. Therefore it is difficult to quantify the response in $W_{tot}$ with applied power, however the qualitative response is evident.

## 4. Reconstruction quality of NSTX plasmas

NSTX experimental equilibrium reconstructions typically utilized data from more than 70 magnetic diagnostics including currents from the ohmic heating coil and up to 8 shaping coils (7 independent current measurements), 42 magnetic flux loops, 9 loop voltage monitors, 16 integrated local dB/dt pickup coils, and a Rogowski coil measuring the total toroidal current in the plasma, vacuum vessel, and copper stabilizer plates.

An ensemble of 1500 EFIT reconstructions was run to examine the analysis for large systematic mismatches between experimentally measured and reconstructed signals. These reconstructions comprise the time evolution of 7 different NSTX discharges, beginning at t = 25 ms (when the plasma current typically reaches 100 kA - approximately one-half of the vessel current) until discharge termination. These discharges spanned a large range of plasma parameters and included a plasma heated with HHFW power.

The results are summarized in Table 1. The average absolute and relative errors are given for each measurement group, along with the mean $\xi_j \equiv 1/N\ \Sigma((M_i - C_i) / \varepsilon_{i,j})$ and mean $\xi_j^2 \equiv 1/N\ \Sigma(((M_i - C_i) / \varepsilon_{i,j})^2)$. Here, $M_i$ and $C_i$ are the measured and reconstructed values, respectively, and N is the number of reconstructions. Also, $\varepsilon_{i,j} \equiv (A_j^2 + (R_j \times M_i)^2)^{1/2}$ is the error associated with each measurement, with $A_j$ and $R_j$ being absolute and relative errors, respectively.

| Signal Group | Mean error | | Mean | |
|---|---|---|---|---|
| | Absolute | Relative | $\xi$ | $\xi^2$ |
| OH / shaping coils | 38.9 A | 0.56 % | -0.04 | 0.01 |
| Flux loops (CS) | 6.3 mWb | 0.96 % | 0.61 | 0.54 |
| Flux loops (other) | 3.9 mWb | 1.22 % | 0.042 | 0.49 |
| Integrated dB/dt coils | 1.0 mWb | 2.27 % | -0.11 | 0.27 |
| Plasma Rogowski | 15 kA | 1.5 % | 0.68 | 0.99 |
| Vessel current | 20 kA | 4.0 % | -0.63 | 0.95 |

*Table 1: Summary of experimental measurement errors and normalized differences between measured and reconstructed signals.*

The table shows that while the errors specified for the signals are low, there are no gross systematic or unexpectedly large random errors. The CS flux loops show a very small systematic error which is primarily caused by mismatch with the OH current. The small systematic tendency of the measured Rogowski current to be greater than the computed value ($\xi = 0.68$) is due to the fitting of the integrated dB/dt coils, which tend to reduce the computed current.

## 5. Acknowledgements

Jon Menard is especially acknowledged for performing the difficult task of providing highly accurate magnetics data essential to this analysis. This research was supported by the U.S. Department of Energy under contracts DE-FG02-99ER54524 and DE-AC0276CH03073.

---

[1] Y.-K. M. Peng and D.J. Strickler, *Nucl. Fusion* 26, (1986) 576.
[2] R. D. Stambaugh, V. S. Chan, R. L. Miller, *et al.*, *Fusion Technology* 33 (1998) 1.
[3] A. Sykes, *et al.*, *Plasma Phys. Contr. Nucl. Fus. Res.* 1 (1994) 719.
[4] A.C. Darke, *et al.*, *Fusion Technol.* 1 (1995) 799.
[5] M. Ono, *et al.*, *Phys. Plasmas* 4 (1997) 1953.
[6] R. Raman, *et al.*, Ò*Coaxial Helicity Injection for the Generation of Non-inductive Current in NSTX*Ó, submitted to this conference.
[7] D. Gates, *et al.*, Ò*Initial Operation of NSTX with Plasma Control*Ó, submitted to this conference.
[8] L. L. Lao, *et al.*, *Nucl. Fusion* 25 (1985) 1611.
[9] J. Menard, E. Fredrickson, D. Gates, *et al.*, Ò*Flux Consumption Optimization and the Achievement of 1 MA Discharges on NSTX*Ó, submitted to this conference.
[10] A. Sykes, *et al.*, *Nucl. Fusion* 32 (1992) 694.
[11] R. Maingi, *et al.*, Ò*Initial Wall Conditioning and Impurity Control Techniques in NSTX*Ó, submitted to this conference.
[12] D. Swain, *et al.*, Ò*Results of High-Harmonic Fast Wave Experiments on NSTX*Ó, submitted to this conference.